

# VISION/GESTURE RECOGNITION USING SPIKING NEURONS

October 10, 2014

By  
Qian Liu  
School of Computer Science

# Contents

<b>Abstract</b>	<b>6</b>
<b>1 Introduction</b>	<b>7</b>
1.1 Aim . . . . .	7
1.2 Why is it important . . . . .	8
<b>2 Background</b>	<b>9</b>
2.1 Posture/Gesture Recognition . . . . .	9
2.2 Biology Aspect . . . . .	11
2.3 Platforms . . . . .	11
2.3.1 Vision Processing Front-ends . . . . .	11
2.3.2 SNNs Back-ends . . . . .	11
2.3.3 SpiNNaker distinguishing features . . . . .	14
<b>3 CNNs Models</b>	<b>16</b>
3.1 Model Description . . . . .	16
3.1.1 Manual Feature Extraction Model . . . . .	17
3.1.2 Combined Convolution Network . . . . .	18
3.2 Training and test . . . . .	19
3.3 Experiments . . . . .	19
<b>4 Recognition on SpiNNaker</b>	<b>22</b>
4.1 Moving to spiking neurons . . . . .	22
4.2 Recorded data test . . . . .	22
4.3 Real-time test . . . . .	23
<b>5 Research Plan</b>	<b>25</b>
5.1 Biology Aspect . . . . .	25

5.2	Tracking . . . . .	25
5.3	HMM for gesture recognition . . . . .	25
<b>6</b>	<b>Conclusion</b>	<b>26</b>
	<b>Bibliography</b>	<b>27</b>

# List of Tables

3.1	Sizes of the convolutional neural networks. . . . .	20
3.2	Recognition results . . . . .	21

# List of Figures

2.1	System overview of the posture recognition platform. The silicon retina connects to the SpiNNaker system through an FPGA board. Spikes from the retina are streamed to the SpiNNaker system through this Spartan-6 FPGA board. The jAER software configures the retina and displays its outgoing spikes through the USB connection. The host sets up the runtime parameters off-line and downloads the network model to the SpiNNaker system. . . . .	12
2.2	System diagram . . . . .	13
2.3	103 Machine PCB . . . . .	14
3.1	Each individual convolution neuron connects to its respective field using the same kernel. . . . .	16
3.2	The convolutional neural network model with manually selected templates. . . . .	17
3.3	Real parts of the Gabor filters oriented to four directions. . . . .	18
3.4	Five gesture templates . . . . .	18
3.5	The combined convolutional model with trained MLP neurons. . . . .	18
3.6	Neuron responses to the same five gesture videos. . . . .	19
4.1	Snapshots of the real-time gesture recognition system on SpiNNaker.	24

# Abstract

The extraction of the report not the research.

The aim, objectives and motivations are...

What have been done...

The results of experiment...

One sentence about the conclusions and future plan. About half page long.

# Chapter 1

## Introduction

In order to make an effective, energy-efficient touch-less user interface (UI), we will model an optimized spiking neural network (SNN) based hand-gesture command identifier on bespoke hardware. The SpiNNaker platform will be employed in the initial stages of research to model and optimize the SNNs in real time, computing the output based on spiking output from a silicon retina: a dynamic visual sensor (DVS). After deriving the neural network description, later work will focus on specifying the minimum number of neurons to operate it.

The SpiNNaker project (funded by EPSRC, the UK funding agency for engineering and the physical sciences) has supported the development of an experimental multicore platform that offers a unique environment for research into many-core programming. SpiNNaker employs an architecture inspired by the very high levels of connectivity found in the human brain, and the primary objective of the research has been to develop a generic platform for real-time brain modelling. The resulting machine is a mesh of Multi-Processor Systems-on-Chip (MPSoCs) that will be scaled up over 2013 within the current funding to machines with up to a million processor cores.

### 1.1 Aim

Goal 1: prototype a neural gesture recognition system on SpiNNaker.

Once the gesture recognition system is functioning effectively the SpiNNaker platform can then be used to explore the optimal spiking neural network size and configuration for the gesture recognition task.

Goal 2: evaluate the cost and performance trade-offs in optimizing the number of neural components required to deliver effective gesture recognition.

Here cost is taken to include a range of measures of the implementation complexity, including the numbers and types of neurons, the numbers and types of synapses, the computational demands which are usually dominated by the number of synaptic connections per second, and the power consumption of the system. Performance is taken to be a measure of the effectiveness of the system at recognizing gestures.

#### Expected Outcomes and Results

The tangible outcomes of the first year of the proposed research will include:

A prototype spiking neuron gesture recognition system running on SpiNNaker.

An understanding of the trade-offs of performance, cost and complexity in a spiking neuron gesture recognition system.

These outcomes will be documented in specific deliverables:

A paper submitted to a leading conference such as ICANN.

A draft patent application.

## **1.2 Why is it important**

Why is it important to research on vision process in the brain.



# Chapter 2

## Background

Literature Review

### 2.1 Posture/Gesture Recognition

All the literature review I can borrow from the previous report.

a pattern or an object in a two-dimensional image can be described with four properties [1]: position, geometry (size, area and shape), color and texture, and trajectory. Appearance-based methods are the most direct approaches to perform pattern recognition. The test image is compared with all the templates to find the best match on one particular or a combination of properties. In terms of classification algorithms, distance measure methods (nearest neighbour, k-means clustering), support vector machine (SVM), multi-layer perceptron (MLP) neural networks and statistical methods, e.g. Gaussian mixture model (GMM) have been applied successfully in visual recognition. Since the 2D projection of an object changes under various illuminations, viewing angles, relative positions and distances (size), it is impossible to represent all appearances of an object in different conditions. Robust matching methods are employed, such as edge matching [2], the divide-and-conquer approach [3], gradient matching [4], etc. Moreover, feature based methods are used to improve reliability, robustness and classification efficiency. Among various feature extraction methods, the scale-invariant feature transform (SIFT) [5] and the sped-up robust features (SURF) [6] methods are well-accepted recently in the field. However, to find a proper feature for a specific object still remains an open question and there is not any process as accurate, general and effective as the brain. Turning to biology for answers is always the way to explore the field of visual pattern recognition. Riesenhuber and Poggio [7] presented a

biologically-inspired model following the organization of the visual cortex which has the ability to represent relative position- and scale-invariant features. Integrating a rich set of visual features became available using a feed-forward hierarchical pathway.

More and more attention has been drawn into the investigation of spiking neural networks for vision processing. Pattern information can be encoded in the delays between the pre- and post-synaptic spikes since the spiking neurons are capable of computing radial basis functions (RBFs) [8]. A further study [9] has stated that spatio-temporal information can be also stored in the exact firing time instead of the relative delay. Maass [10] has proved mathematically that: 1) networks of spiking neurons are computationally more powerful than the first and second generation of neural network models; 2) a concrete biologically relevant function can be computed by a single spiking neuron, replacing hundreds of hidden units in a sigmoidal neural net; 3) any function that can be computed by a small sigmoidal neural net can also be computed by a small network of spiking neurons. Applications of SNN-based vision processing have been successfully carried out. A two-layered SNN has been trained using spike time dependent plasticity (STDP) and employed for a character recognition task [11]. Lee and co-authors [12] have implemented the direction selective filters in real time using spiking neurons. The direction selective filters here are considered as a layer of convolution module in the model of so called convolution neural network [13]. Different features, such as Gabor filter features (scale, orientation and frequency) and shape can be modelled as layers of feature maps. Rank order coding, as an alternative to conventional rate-based coding, treats the first spike the most important and has well applied to an orientation detection training process [14]. Nengo [15] is a graphical and scripting based software package for simulating large-scale neural systems and has been used to build the world's largest functional brain model, Spaun [16]. An FPGA implementation of a Nengo model for digit recognition has been reported [17]. Deep Belief Networks (DBNs), the 4th generation of artificial neural network, has shown a strong ability in solving classification problems. A recent study [18] has resoundingly mapped an offline-trained DBN onto an efficient event-driven spiking neural network for a digit recognition task. Hand segmentation and feature extraction usually takes the colour into account and involves wavelets, e.g. using a Kalman filter. Thus, shape-only recognition of the hand posture will be a challenge. In the terms of gesture recognition, the hidden Markov model (HMM) has shown its ability to recognize dynamic gestures [19]. However, with their instinctive temporal processing, SNNs have the potential to deliver dynamic gesture recognition.

## 2.2 Biology Aspect

A lot to work on this part. May or may not include neuron models.

## 2.3 Platforms

This section presents some details of the two hardware components, the Address-Event Representation (AER) silicon retina [20] and the SpiNNaker system [21] which is a massive parallel computing platform aimed at real-time simulation of spiking neural networks (SNNs). Figure 2.1 shows the combined hand posture recognition system; the AEREAR2 silicon retina connected to the SpiNNaker 48-node board via a Spartan 6 FPGA board [22]. The jAER [23] event-based processing software<sup>1</sup> running on the PC configures the retina and displays the output spikes through a USB link. The host communicates to the SpiNNaker board via Ethernet to set up its runtime parameters and to download the neural network model off-line and uses a visualiser [24] to show the spiking activities in real-time.

### 2.3.1 Vision Processing Front-ends

The visual front-end is constituted by a Dynamic Video Sensor (DVS) silicon retina, an asynchronous sensor which provides spike events encoding the address of pixels undergoing a contrast change[4]. This approach lies in opposition to the more traditional method of sending entire frames to provide fast ( $3\ \mu\text{s}$  latency) data-driven contrast detection at a wide range of illuminations. The sensor is capable of transmitting from 1 Keps to 20 Meps (events per second).

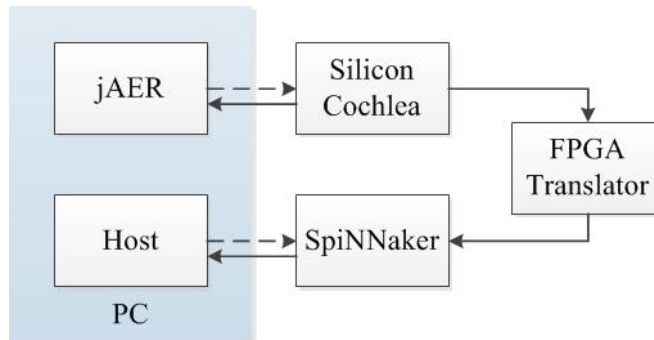
### 2.3.2 SNNs Back-ends

The SpiNNaker project's architecture mimics the human brain's biological structure and functionality. This offers the possibility of utilizing massive parallelism and redundancy to provide resilience in an environment of unreliability and failure of individual components.

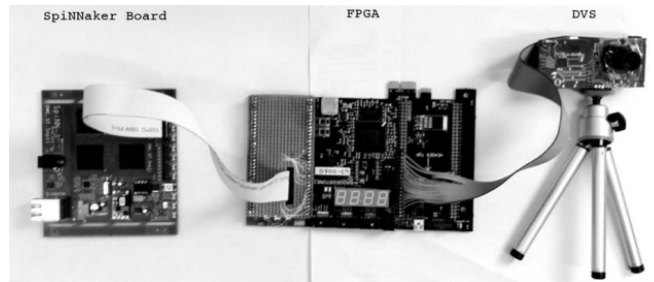
In the human brain, communication between its computing elements, or neurons, is achieved by the transmission of electrical "spikes" along connecting axons. The biological processing of the neuron can be modelled by a digital processor and the axon

---

<sup>1</sup><http://sourceforge.net/p/jaer/wiki/Home/>



(a) Outline of the platform



(b) Picture of the hardware platform

Figure 2.1: System overview of the posture recognition platform. The silicon retina connects to the SpiNNaker system through an FPGA board. Spikes from the retina are streamed to the SpiNNaker system through this Spartan-6 FPGA board. The jAER software configures the retina and displays its outgoing spikes through the USB connection. The host sets up the runtime parameters off-line and downloads the network model to the SpiNNaker system.

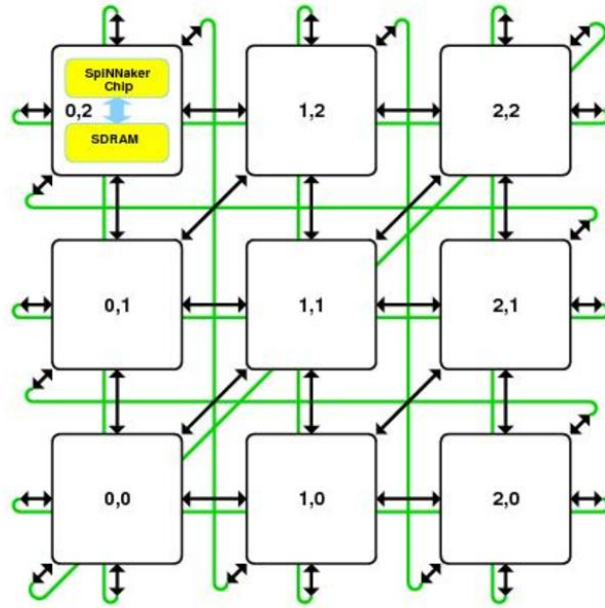


Figure 2.2: System diagram

connectivity can be represented by messages, or information packets, transmitted between a large number of processors which emulate the parallel operation of the billions of neurons comprising the brain.

The engineering of the SpiNNaker concept is illustrated in the Figure 2.2 where the hierarchy of components can be identified. Each element of the toroidal interconnection mesh is a multi-core processor known as the "SpiNNaker Chip" comprising 18 processing cores. Each core is a complete processing sub-system with local memory and a DMA capability. It is connected to its local peers via a Network-on-Chip (NoC) which provides local high bandwidth communication and to other SpiNNaker chips via links between SpiNNaker chips. In this way the massive parallelism extending to thousands or millions of processors is possible.

The knowledge content and learning ability of the brain is embodied in its evolvable interconnection pattern; this routes a spike generated by one neuron to others which are interconnected with it by axons and these interconnections are modified and extended as a result of the learning and processes.

In SpiNNaker a packet Router within each multi-core processor controls the neural interconnection. Each transmitted packet representing a spike contains information which identifies its source neuron; this is used by a multi-core processor's Router to

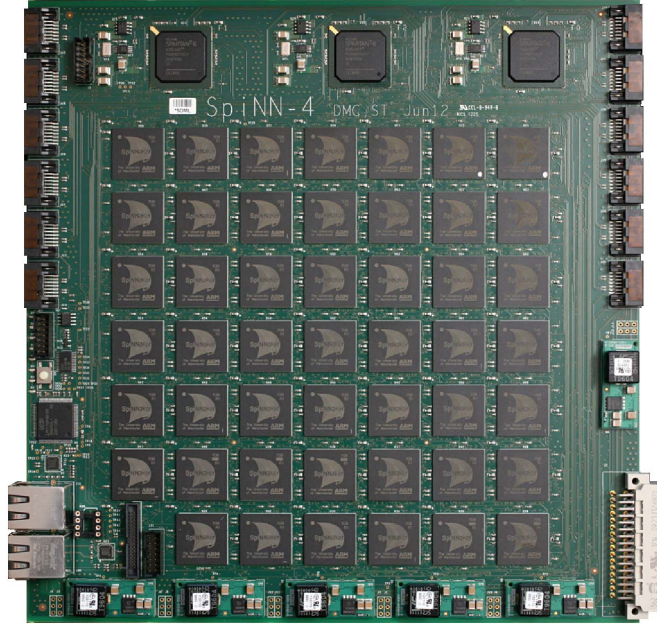


Figure 2.3: 103 Machine PCB

identify whether this packet should be routed to one of its contained application processors to respond, or should be routed on to one of the six adjacent multi-core processors connected to it as part of the overall SpiNNaker network.

The 103 machine is the 48-node board, see Figure 2.3, and has 864 ARM processor cores, typically deployed as 768 application cores, 48 Monitor Processors and 48 spare cores. The 103 machine requires a 12V 6A supply. The control interface is two 100Mbps Ethernet connections, one for the Board Management Processor and the second for the SpiNNaker array. There are options to use the nine on-board 3.1Gbps high-speed serial interfaces (using SATA cables, but not necessarily the SATA protocol) for I/O; this will require suitable configuration of the on-board FPGAs that provide the high-speed serial interface support. 103 boards can be connected together to form larger systems using the high-speed serial interfaces.

### 2.3.3 SpiNNaker distinguishing features

Interfacing AER Sensors:

Spikes from the silicon retina are injected to SpiNNaker through one of the 6 bi-directional on-board links by a SPARTAN-6 FPGA board that translates them into a SpiNNaker compatible AER format<sup>2</sup>. From the software point of view, interfacing the

<sup>2</sup>AppNote 8 - Interfacing AER devices to SpiNNaker using an FPGA.

silicon retina can be done using pyNN. The user sets a Spike Source population that resides on a virtual SpiNNaker chip, to which an AER sensor's spikes are directed, thus abstracting away the hardware details from the users[22].

# Chapter 3

## CNNs Models

The convolutional neural network (CNN) is well-known as an example of a biologically-inspired model. The repeated convolutional kernels are overlapped in the receptive fields of the input neurons. Figure 3.1 shows a typical convolutional connection between two layers of neurons.

### 3.1 Model Description

There are two CNNs proposed to accomplish the posture recognition task. A straight forward method of template matching was employed at first, and then a multi-layer perceptrons (MLP) was trained to improve the recognition performance.

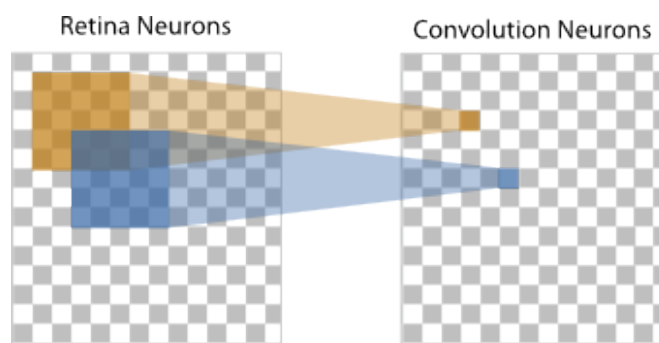


Figure 3.1: Each individual convolution neuron connects to its respective field using the same kernel.



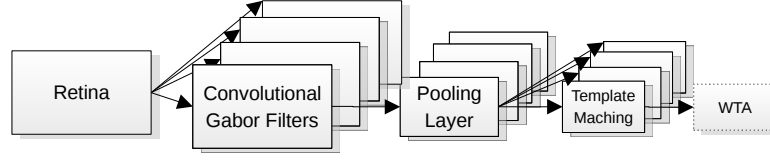


Figure 3.2: The convolutional neural network model with manually selected templates.

### 3.1.1 Manual Feature Extraction Model

Shown in Figure 3.2 the first two layers are the input layer and the convolution layer, where the kernels are Gabor filters responding to four orientations. The third layer is the pooling layer where the size of the populations shrinks. This down-sampling enables robust classification due to its tolerance to variations in the precise shape of the input. The fourth layer is another convolution layer where the output from the pooling layer is convolved with the templates. Each template is a frame (one frame consists of 30ms of spiking activity) of output spikes from the pooling layer. The Gabor filter is well-known as a linear filter for edge detection in image processing. A Gabor filter is a 2D convolution of a Gaussian kernel function and a sinusoidal plane wave; see Equation 3.1.  $\theta$  represents the orientation of the filter,  $\lambda$  is the wavelength of the sine wave, and  $\sigma$  is the standard deviation of the Gaussian envelope. The frequency and orientation features are similar to the responses of V1 neurons in the human visual system. Only the real parts of the Gabor filters (see Figure 3.3) are used as the convolutional kernels to configure the weights between the input layer and the Gabor filter layer.

$$RealParts = \exp\left(\frac{-x'^2 + y'^2}{2\sigma^2}\right) \cos(2\pi \frac{x'}{\lambda})$$

$$ImaginaryParts = \exp\left(\frac{-x'^2 + y'^2}{2\sigma^2}\right) \sin(2\pi \frac{x'}{\lambda})$$

$$where : \tag{3.1}$$

$$x' = x \cos(\theta) + y \sin(\theta)$$

$$y' = -x \sin(\theta) + y \cos(\theta)$$

The templates (see Figure 3.4) are manually selected from the output of the pooling layer in the framed Matlab simulation. The output score of a convolution neuron is higher when its receptive field matches a certain template more. There are five populations of template matching neurons for five gestures in our system. The activity of

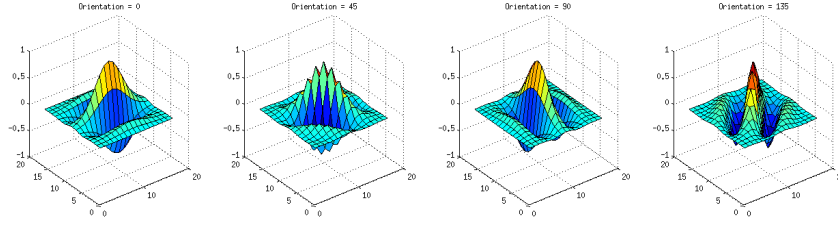


Figure 3.3: Real parts of the Gabor filters oriented to four directions.

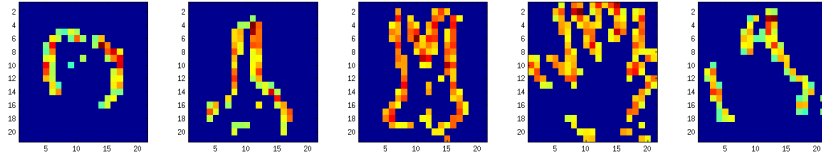


Figure 3.4: Five gesture templates

the template matching populations indicates naturally the position of the gestures.

**Biology background on V1, especially for Gabor Filters.**

### 3.1.2 Combined Convolution Network

Inspired by the research of Lecun [25] and etc., we designed a combined network model with MLP and the convolutional network (Figure 3.5). Thanks to the help of tracking, only the most active region in the pooling layer is forwarded to the next layer. A trained static 3-layered MLP is attached to classify the gesture.

Since the size of the input image of the MLP training is fixed and the position is centered, tracking plays a very important role to spot the valid region. Tracking is naturally embedded in the pooling layer of the convolutional network, for the active neurons directly point out the lively receptive field. **However, to extract only the active region to the next layer is still need to investigate.**

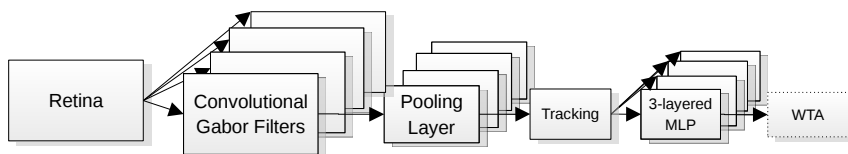


Figure 3.5: The combined convolutional model with trained MLP neurons.

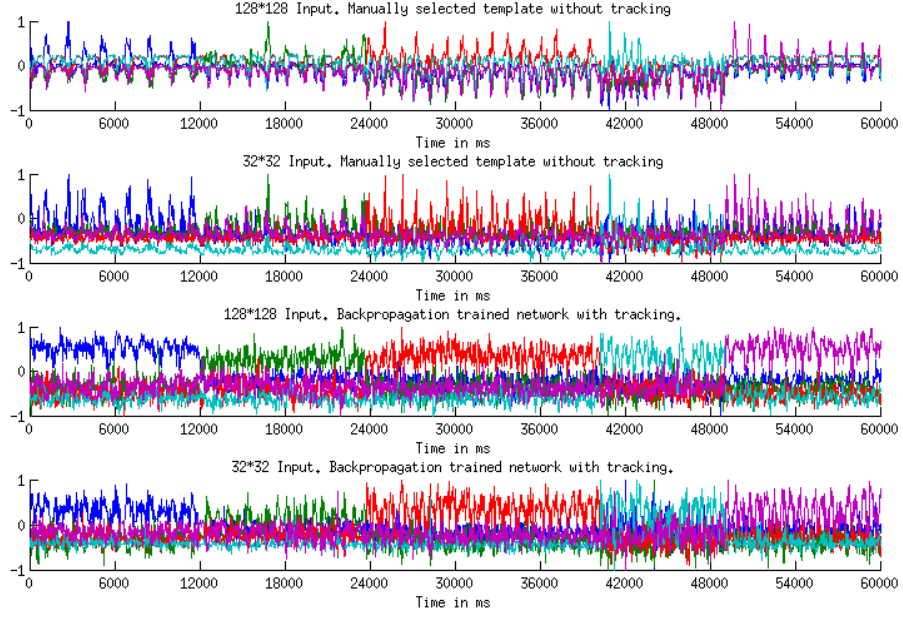


Figure 3.6: Neuron responses to the same five gesture videos.

## 3.2 Training and test

Training is missing here.

In order to evaluate the cost and performance trade-offs in optimizing the number of neural components, both the convolutional models described above were tested at different sizes. Five gesture videos were captured from the silicon retina in address-event representation (AER [26]) format. All the gestures are of similar size and moving clock-wise in front of the retina. The videos are cut into frames (30ms/frame) and push forward into the convolutional networks. The configurations of the networks are listed in Table 3.1 (Model 1: template matching; Model 2: trained MLP). The integration layer is not necessary in a convolutional network, it is used here to fit the template matching and decrease the number of synaptic connections.

## 3.3 Experiments

In Figure 3.6 the first two plots refer to Model 1, using template matching. Each colour represents one of the recognition populations. Each point in the plot is the highest neuronal response in the recognition population during the time of one frame (30 ms).

Table 3.1: Sizes of the convolutional neural networks.

(a) Model 1: Template matching

	<b>Full Resolution</b>		<b>Sub-sampled Resolution</b>	
	Neuron Number	Connections per Neuron	Neuron Number	Connections per Neuron
<b>Retinal Input</b>	$128 \times 128$	1	$32 \times 32$	$4 \times 4$
<b>Gabor Filter</b>	$112 \times 112 \times 4$	$17 \times 17$	$28 \times 28 \times 4$	$5 \times 5$
<b>Pooling Layer</b>	$36 \times 36 \times 4$	$5 \times 5$	null	null
<b>Integration Layer</b>	$36 \times 36$	4	$28 \times 28$	4
<b>Template Matching</b>	$16 \times 16 \times 5$	$21 \times 21$	$14 \times 14 \times 5$	$15 \times 15$
<b>Total</b>	74320	15216512	5925	318420

(b) Model 2: Trained MLP network layers after tracking

	<b>Full Resolution</b>		<b>Sub-sampled Resolution</b>	
	Neuron Number	Connections per Neuron	Neuron Number	Connections per Neuron
<b>Tracked Input</b>	$21 \times 21$	null	$15 \times 15$	null
<b>Hidden Layer</b>	10	$21 \times 21 \times 10$	10	$15 \times 15 \times 10$
<b>Recognition Layer</b>	5	$5 \times 10$	5	$5 \times 10$
<b>Total</b>	456	4460	240	2300

Table 3.2: Recognition results

		Model 1		Model 2	
		High Resolution	Low Resolution	High Resolution	Low Resolution
<b>Fist</b> (399 Frames)	Correct	99.11%	99.23%	96.24%	84.21%
	Reject	71.93%	67.42%	Null	Null
<b>One Finger</b> (392 Frames)	Correct	92.98%	80.00%	94.39%	71.69%
	Reject	70.92%	75.77%	Null	Null
<b>Victory Sign</b> (551 Frames)	Correct	96.56%	93.07%	95.64%	87.66%
	Reject	73.68%	81.67%	Null	Null
<b>Full Hand</b> (293 Frames)	Correct	95.65%	72.41%	93.52%	72.01%
	Reject	92.15%	90.10%	Null	Null
<b>Thumb up</b> (391 Frames)	Correct	89.61%	84.44%	96.68%	74.68%
	Reject	80.31%	76.98%	Null	Null

The neuronal response, the spiking rate, is normalized to  $[-1, 1]$ . It can be seen that the higher resolution input makes the boundaries between the classes clearer. On the other hand, recognition only happens when the test image and template are similar enough. The templates are only selected from the frames where the gestures are moving towards the right, and the gestures are moving clockwise in the videos. Thus, all the peaks in plot 1 signify that the direction of the gestures movement is right. It is notable that the higher resolution causes the recogniser to be more sensitive to the differences between the test data and the template, while the smaller neural network can recognize more generalized patterns. Therefore, a threshold is required to differentiate between data that is close enough and that which is not. Since the gestures are moving in four different directions during the clockwise movement, a rejection rate of 75% is to be expected. The latter two plots refer to Model 2. The three-layer MLP network significantly improves the recognition rate and can generalize the pattern. There is no rejection rate for Model 2. The detailed results are listed in Table 3.2. The correct recognition rate is calculated from the non-rejected frames. The lower resolution of the  $32 \times 32$  retina input is adequate for this gesture recognition task. The smaller network uses only 1/10 the number of neurons and 1/50 the number of synaptic connections compared to the full resolution network, while the recognition rate drops only around 10% with Model 1 and 15% with Model 2.

# Chapter 4

## Recognition on SpiNNaker

### 4.1 Moving to spiking neurons

Mathematical approach. Need to work hard on.

It remains a challenge to map the weights of a traditional artificial neural network to a spiking neural network. There are attempts to estimate the rate of Leaky integrate-and-fire (LIF) neurons with Poisson input spike trains [27]. For the model illustrated above, there are two types of synaptic connection: one-to-one connections in the retina layer and N-to-one connections in all the convolutional layers (the pooling layer is also included). For the retina layer, 1) the problem is: what is the connection weight between two single LIF neurons to make a post-synaptic neuron fire whenever the pre-synaptic neuron generates a spike? While for the convolutional neurons, 2) given the input spike rates, LIF neuron parameters and the output spiking rate, what are the corresponding weights between the two layers? [In terms of the main goals of the report, the detailed mathematical reasoning will be demonstrated in the paper which will be submitted in November. A lot of work to be done here.](#)

### 4.2 Recorded data test

New experiment to work on.

New tool need to be fixed (Spike Source Array), and maybe new ways of reloading.

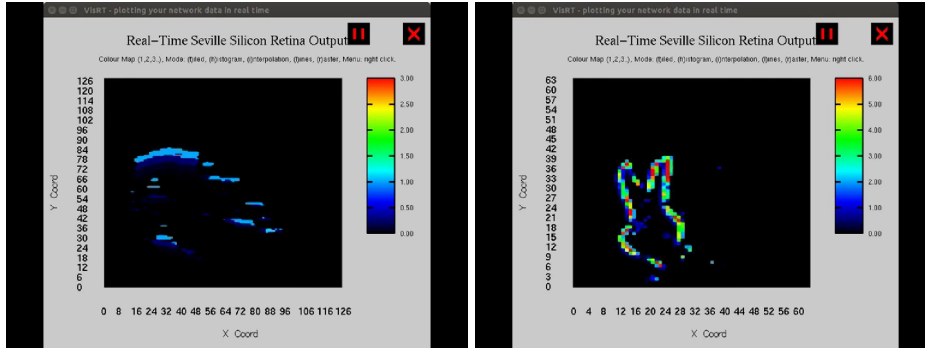
## 4.3 Real-time test

We implemented the prototype of the neural gesture recognition system on SpiNNaker. The input retina layer consists of  $128 \times 128$  neurons; each Gabor filter has  $112 \times 112$  valid neurons, since the kernel size is  $17 \times 17$ ; each pooling layer is as big as  $36 \times 36$ , convolving with five template kernels ( $21 \times 21$ ); thus, the recognition populations are  $16 \times 16$  neurons each. Altogether 74,320 neurons and 15,216,512 synapses use up to 19 chips on a 48-node board.

Figure 4.1 shows snapshots of the real time gesture recognition system. Figure 4.1a is a snapshot of the Gabor filter layer, where Figure 4.1b shows the integration of all the pooled populations, and the active neurons in the visualizer in Figure 4.1c are pointing out the position of the recognized pattern (One finger). All the videos can be found on Youtube<sup>1</sup>.

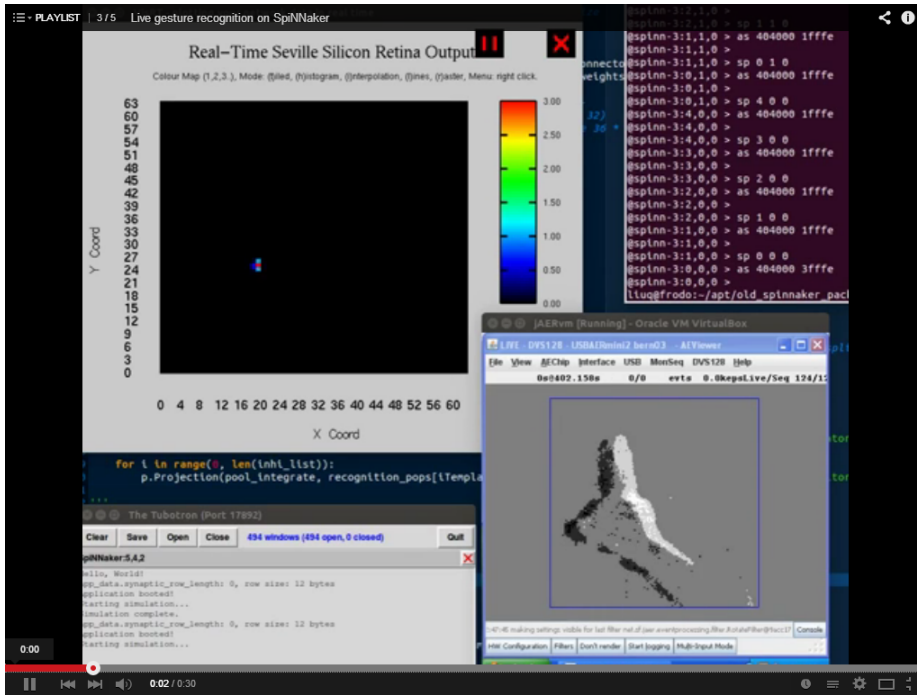
---

<sup>1</sup><http://youtu.be/PvJy6RKAJhw?list=PLxZ1W-Upr3eoQuLxq87qpUL-CwSphtEBJ>, <http://youtu.be/FZJshPCJlpg?list=PLxZ1W-Upr3eoQuLxq87qpUL-CwSphtEBJ>, <http://youtu.be/yxN90aGGKvg?list=PLxZ1W-Upr3eoQuLxq87qpUL-CwSphtEBJ>



(a) Outline of the platform

(b) Picture of the hardware platform



(c) Picture of the hardware platform

Figure 4.1: Snapshots of the real-time gesture recognition system on SpiNNaker.



## **Chapter 5**

### **Research Plan**

#### **5.1 Biology Aspect**

#### **5.2 Tracking**

#### **5.3 HMM for gesture recognition**

# **Chapter 6**

## **Conclusion**

Just a conclusion

# Bibliography

- [1] S. G. Wysocki, L. Benuskova, and N. Kasabov, “Fast and adaptive network of spiking neurons for multi-view visual pattern recognition,” *Neurocomputing*, vol. 71, no. 13, pp. 2563–2575, 2008.
- [2] J. Canny, “A computational approach to edge detection,” *Pattern Analysis and Machine Intelligence, IEEE Transactions on*, no. 6, pp. 679–698, 1986.
- [3] Ö. Toygar and A. Acan, “Multiple classifier implementation of a divide-and-conquer approach using appearance-based statistical methods for face recognition,” *Pattern Recognition Letters*, vol. 25, no. 12, pp. 1421–1430, 2004.
- [4] S.-D. Wei and S.-H. Lai, “Robust and efficient image alignment based on relative gradient matching,” *Image Processing, IEEE Transactions on*, vol. 15, no. 10, pp. 2936–2943, 2006.
- [5] D. G. Lowe, “Distinctive image features from scale-invariant keypoints,” *International journal of computer vision*, vol. 60, no. 2, pp. 91–110, 2004.
- [6] H. Bay, A. Ess, T. Tuytelaars, and L. Van Gool, “Speeded-up robust features (surf),” *Computer vision and image understanding*, vol. 110, no. 3, pp. 346–359, 2008.
- [7] M. Riesenhuber and T. Poggio, “Hierarchical models of object recognition in cortex,” *Nature neuroscience*, vol. 2, no. 11, pp. 1019–1025, 1999.
- [8] J. J. Hopfield, “Pattern recognition computation using action potential timing for stimulus representation,” *Nature*, vol. 376, no. 6535, pp. 33–36, 1995.
- [9] T. Natschläger and B. Ruf, “Spatial and temporal pattern analysis via spiking neurons,” *Network: Computation in Neural Systems*, vol. 9, no. 3, pp. 319–332, 1998.

- [10] W. Maass, “Networks of spiking neurons: the third generation of neural network models,” *Neural networks*, vol. 10, no. 9, pp. 1659–1671, 1997.
- [11] A. Gupta and L. N. Long, “Character recognition using spiking neural networks,” in *Neural Networks, 2007. IJCNN 2007. International Joint Conference on*, pp. 53–58, IEEE, 2007.
- [12] J. H. Lee, P. Park, C.-W. Shin, H. Ryu, B. C. Kang, and T. Delbruck, “Touchless hand gesture ui with instantaneous responses,” in *Image Processing (ICIP), 2012 19th IEEE International Conference on*, pp. 1957–1960, Sept 2012.
- [13] L. Camunas-Mesa, C. Zamarreno-Ramos, A. Linares-Barranco, A. J. Acosta-Jimenez, T. Serrano-Gotarredona, and B. Linares-Barranco, “An event-driven multi-kernel convolution processor module for event-driven vision sensors,” *Solid-State Circuits, IEEE Journal of*, vol. 47, no. 2, pp. 504–517, 2012.
- [14] A. Delorme, L. Perrinet, and S. J. Thorpe, “Networks of integrate-and-fire neurons using rank order coding b: spike timing dependent plasticity and emergence of orientation selectivity,” *Neurocomputing*, vol. 38, pp. 539–545, 2001.
- [15] C. Eliasmith and T. C. Stewart, “Nengo and the neural engineering framework: connecting cognitive theory to neuroscience,” in *Proceedings of the 33rd annual meeting of the cognitive science society*, pp. 1–2, 2011.
- [16] C. Eliasmith, T. C. Stewart, X. Choo, T. Bekolay, T. DeWolf, Y. Tang, and D. Rasmussen, “A large-scale model of the functioning brain,” *science*, vol. 338, no. 6111, pp. 1202–1205, 2012.
- [17] M. Naylor, P. J. Fox, A. T. Markettos, and S. W. Moore, “Managing the fpga memory wall: Custom computing or vector processing?,” in *Field Programmable Logic and Applications (FPL), 2013 23rd International Conference on*, pp. 1–6, IEEE, 2013.
- [18] P. O’Connor, D. Neil, S.-C. Liu, T. Delbruck, and M. Pfeiffer, “Real-time classification and sensor fusion with a spiking deep belief network,” *Frontiers in neuroscience*, vol. 7, 2013.
- [19] M. Elmezain, A. Al-Hamadi, J. Appenrodt, and B. Michaelis, “A hidden markov model-based isolated and meaningful hand gesture recognition,” *International*

- Journal of Electrical, Computer, and Systems Engineering*, vol. 3, no. 3, pp. 156–163, 2009.
- [20] J. A. Leñero-Bardallo, T. Serrano-Gotarredona, and B. Linares-Barranco, “A 3.6 s latency asynchronous frame-free event-driven dynamic-vision-sensor,” *Solid-State Circuits, IEEE Journal of*, vol. 46, no. 6, pp. 1443–1455, 2011.
  - [21] S. B. Furber, F. Galluppi, S. Temple, and L. A. Plana, “The spinnaker project,” 2014.
  - [22] F. Galluppi, K. Brohan, S. Davidson, T. Serrano-Gotarredona, J.-A. P. Carrasco, B. Linares-Barranco, and S. Furber, “A real-time, event-driven neuromorphic system for goal-directed attentional selection,” in *Neural Information Processing*, pp. 226–233, Springer, 2012.
  - [23] T. Delbruck, “Frame-free dynamic digital vision,” in *Proceedings of Intl. Symp. on Secure-Life Electronics, Advanced Electronics for Quality Life and Society*, pp. 21–26, 2008.
  - [24] C. Patterson, F. Galluppi, A. Rast, and S. Furber, “Visualising large-scale neural network models in real-time,” in *Neural Networks (IJCNN), The 2012 International Joint Conference on*, pp. 1–8, 2012.
  - [25] Y. LeCun, L. Bottou, Y. Bengio, and P. Haffner, “Gradient-based learning applied to document recognition,” *Proceedings of the IEEE*, vol. 86, no. 11, pp. 2278–2324, 1998.
  - [26] J. Lazzaro and J. Wawrzynek, “A multi-sender asynchronous extension to the aer protocol,” in *Advanced Research in VLSI, Conference on*, pp. 158–158, IEEE Computer Society, 1995.
  - [27] G. La Camera, M. Giugliano, W. Senn, and S. Fusi, “The response of cortical neurons to in vivo-like input current: theory and experiment,” *Biological cybernetics*, vol. 99, no. 4-5, pp. 279–301, 2008.